Jan Bonarski
Institute of Metallurgy and Materials Science
Polish Academy of Sciences, Kraków

ON FUNCTIONALLY GRADED MATERIALS. TEXTURE TOMOGRAPHY

Key words

tomography, X-ray diffraction, functionally graded material

Abstract

The study gives a review of a functionally graded material (FGM) and non-conventional investigation its inhomogeneous structure. The FGMs are a new class of high-performance composite materials in which two or more constituent phases occur in continuously varying spatial distributions that are responsive to functional performance requirements. FGMs eliminate the sharp discontinuities in material composition that occur in classical composites, thereby minimizing stress concentrations and maximizing performance.

Among phenomena determining the FGM properties a crucial role plays its anisotropy. One of the most effective characteristics in this field is a crystallographic texture which describes the space organization of microstructure. However, respecting a subtle system of residual stresses, liability of lattice modifications, meta-stability of phases, and so on, a non-destructive research tool for investigation of the inhomogeneous

microstructure of the FGM is required. Such a tool becomes an advanced method termed as X-ray Texture Tomography (XTT). The method consists in estimation of crystallographic texture through the thickness of a near-surface area of determined constructing element. Both, principles and effectiveness of the XTT method for determination of texture depth-profile of the FGM-made layers are also presented in the study. The nature of texture formation in the novel class of material (FGMs) is discussed.

Streszczenie

Przedstawiono przegląd funkcjonalnych materiałów gradientowych (FMG) i niekonwencjonalną metodę analizy ich niejednorodnej struktury. FMG stanowią nowy rodzaj materiałów kompozytowych o podwyższonych właściwościach, w których dwie lub więcej faz składowych wykazuje ciągłą zmianę ilościowego udziału odpowiedzialną za właściwości funkcjonalne. W materiałach tych wyeliminowane jest skokowe przejście nieciągłości strukturalnych obserwowane w konwencjonalnych materiałach kompozytowych, minimalizując w ten sposób koncentrację naprężeń, a podnosząc właściwości eksploatacyjne.

Anizotropia odgrywa kluczową rolę wśród różnych właściwości charakteryzujących FMG, zaś jedną z najbardziej odpowiedzialnych charakterystyk jest tekstura krystalograficzna, opisująca przestrzenny rozkład właściwości mikrostruktury. Do innych czynników odgrywających rolę zalicza się dyskretny rozkład naprężeń, zmiany parametru sieciowego, metastabilność faz i inne. Narzuca to konieczność wykorzystania nieniszczących metod do diagnostyki niejednorodności struktury FMG. Narzędziem takim jest rentgenowska tomografia teksturowa bazująca na wyznaczeniu zmian uprzywilejowanej orientacji krystalograficznej na grubości elementów

konstrukcyjnych w obszarze przypowierzchniowym. Podstawy oraz wykorzystanie tej metody zostały przedstawione w pracy w zastosowaniu do wyznaczenia profilu zmian tekstury w warstwach FMG. Rozważane zostały przyczyny tworzenia się tekstury w tej nowej grupie FMG.

Functionally graded material

Functionally graded material (FGM) is a macroscopically inhomogeneous composite material that has a gradient in composition from one surface to another (*Panda and Ravi Chandran, 2003*)[11]. FGM is a two- or multi-component composite characterised by a compositional gradient from one component(s) to the other. In contrast, traditional composites are homogeneous mixtures, and they therefore involve a compromise between the desirable properties of the component materials. Since significant proportions of an FGM contain the pure form of each component, the need for compromise is eliminated. The properties of the components can be fully utilised. For example, the toughness of a metal can be accompanied with the refractoriness of a ceramic, without any compromise in the toughness of the metal side or the refractoriness of the ceramic side.

FGMs are applied more and more frequently in advanced technologies of materials engineering and since introduction of its concept in the early 1990s, many research programs were devoted to this subject. Gradient materials have historically been used throughout the world to solve difficult problems in joining materials differing in coefficients of thermal expansion (CTE). This differential CTE is particularly troublesome when the materials must be joined at elevated

temperatures or must be used at elevated temperatures. It is known that direct bonding of the metal and the ceramic generates thermal stresses due to the CTE mismatch and often leads to cracking of the ceramic, thus making the bi-materials unsuitable for structural use.

Glass-to-metal and quartz-to-metal seals are examples where gradient joints were in use more than forty years ago. By gradually changing the glass composition at the glass-metal joint a seal could be formed which would survive the hot forming process. This process was later used in the 1960's to form high temperature ceramic-to-metal seals. A gradient *cer-met* layer with a high metal content on the metal side and a high ceramic content on the ceramic side overcame the problems of CTE mismatch in these ceramic-to-metal seals.

A revival of the world's interest in gradient materials began the Japanese in 1984 during the space-plane project, in the form of a proposed thermal barrier material capable of withstanding a surface temperature of 2000 K and a temperature gradient of 1000 K across a cross section < 10 mm. The next national project called "Research on the Basic Technology for the Development of Functionally Gradient Materials (FGM) for Relaxation of Thermal Stress" undertaken in 1987 opened a comprehensive research period and initiated a commercial reality in the field of the FGM (*Holt et al., 1993*)[7].

FGMs are now being evaluated to solve more than just CTE mismatch problems. They are being evaluated as a means of altering the mechanical, thermal, acoustic, electrical, or optical properties of composite materials. Altering these materials properties requires

changing the chemical composition, microstructure, state, distribution pattern or other factors in the FGM layer interface between materials. These changes can take place over a relatively short distance, or over the entire length of the component being fabricated. In the sense, a nitrided steel, for instance, could be also regarded as a FGM.

In an ideal FGM, the material properties may vary smoothly in one dimension (e.g., are constant in (x,y) but vary with z). As an example, having a smooth transition region between a pure metal and pure ceramic would result in a material that combines the desirable high temperature properties and thermal resistance of a ceramic, with the fracture toughness of a metal (see Fig. 1).

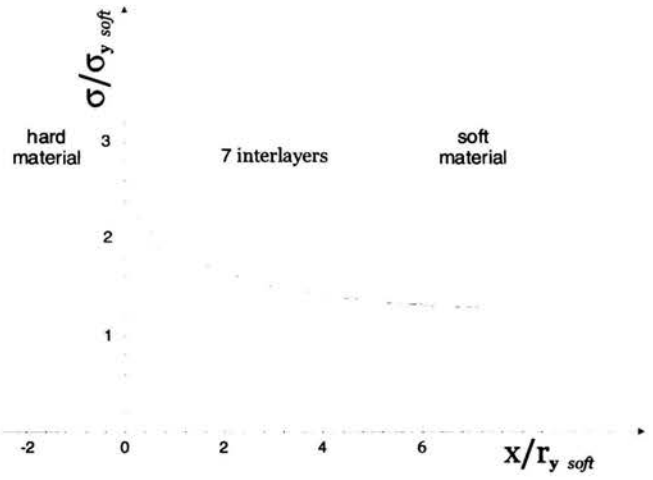

Fig. 1. *Transition of a hard surface layer to a soft base material divided into the seven layers. The yield stress (σ_y) and thickness of the seven intermediate layers was optimized so that, for a crack in the surface layer, the crack driving force, i.e., the tendency of the crack to grow into the base material is as small as possible (modeling of the fracture behavior of inhomogeneous materials is applied). $r_{y,soft}$ is the radius of the plastic zone in the base material, x is the distance from the surface layer.*

For providing the continuous thickness-profile of the properties of the FGM-made constructing elements it internal structure should characterizes the following advantages over the interface joints:

— effective reduction in the overall magnitude of the thermal stresses,
— delaying of the plastic yielding and the failure of the metallic layer by the load sharing of the ceramic,
— better overall use of the available materials by distributing them in a suitable spatial direction.

The concept of FGM was conceived also for long-term use in applications involving high operational temperatures and large temperature gradients such as that in aerospace. Some of the potential FGM applications include coatings using graded composites of, e.g. *Mo-Si_3N_4*, cutting tools using *WC-Co* graded microstructure, and functional gradient *Ti-Co* materials as dental implants. The FGM system based on *Ti-TiB* is of considerable interest for armor and ballistic applications. This is based on the possibility that *TiB*, being a hard ceramic, can resist the penetration of high velocity projectiles and *Ti*, being a ductile metal, can serve as a back-face absorber structure.

Modern FGMs are constructed for complex requirements, such as the heat shield of a rocket or implants for humans. The gradual transition between the heat or corrosion resistant outer layer (often made of a ceramic material) and the tough metallic base material increases in most cases the life time of the component. Spatially varied microstructures of the FGMs can be accomplished, e.g. through *non-uniform* distribution of

the reinforcement phase with different properties, sizes and shapes, as well as by interchanging the roles of reinforcement and matrix (base) materials in a continuous manner.

One purpose of such an inter-part FGM zone is to provide a smooth transition between materials which are otherwise incompatible because of their mechanical or chemical properties. Another purpose is as a coating to modify the electrical, thermal, chemical or optical properties of the substrate upon which the FGM is applied. Thus the presently applied FGM serves as a multi-functional constructing material.

Multifunctional materials are composite systems that exhibit useful responses to electrical, optical, magnetic and (or) mechanical stimulus. They allow the compact and economic integration of two or more functions of a mechanical, biological, acoustical, thermal, electrical, magnetic and optical sensory or imitate nature. These types of composites materials and systems are presently in the forefront of materials research receiving worldwide attention.

Potential Applications of FGMs

FGMs are an important area of materials science research, with potentially many important applications, e.g., super-heat resistance materials for thermal barrier coatings and furnace facings, vehicle, and personal body armor, electromagnetic sensors, graded refractive index materials for optics, wear-resistant linings for handling large heavy abrasive ore particles, rocket heat shields, heat exchanger tubes,

thermoelectric generators, heat-engine components, plasma facings for fusion reactors, and electrically insulating metal/ceramic joints. They are also ideal for minimizing thermo-mechanical mismatch in metal-ceramic bonding.

One of the wide and still broadened fields is biomedical applications of the FGMs. Functional gradation is one characteristic feature of living tissue. Bio-inspired materials open new approaches for manufacturing implants for bone replacement. An artificial biomaterial for knee joint replacement has been developed by building a graded structure consisting of ultra-high molecular weight polyethylene (UHMWPE) fibre reinforced high-density polyethylene combined with a surface of UHMWPE. The ingrowth behaviour of titanium implants into hard tissue can be improved by depositing a graded biopolymer coating of fibronectin, collagen with a gradation, derived from the mechanisms occurring during healing in vivo. Recently, a wear resisted and bio-compatible layers, like Ti/TiN, made by the laser deposition technique are intensively developed to improvement the human hart assist devices (valves and hart mimic chamber). Depth-changeable micro structure of the layers qualified them also to the FGM class of material.

Functionally graded porous hydroxyapatite (*HAP*, $Ca10(PO_4)_6(OH)_2$) ceramics can be produced using alternative routes, e.g. sintering of laminated structures of HAP tapes filled with polymer spheres or combining biodegradable polyesters such as polylactide, polylactide-*co*-glycolide and polyglycolide, with carbonated nanocrystalline

hydroxyapatite. *HAP–collagen* scaffolds are an appropriate material for in vitro growth of bone.

However, most of the "extreme environment" applications for FGMs require *bulk FGMs*, i.e., FGMs with gradient breadth in the order of millimeters to centimeters, and with continuous gradient profiles. *Bulk FGMs* remain merely a hypothesis. No commercially viable process has yet been developed to make such a material. While the scientific literature abounds in papers on the modeling of the hypothetical properties of *bulk FGMs*, the few proposed fabrication methods are labour-intensive specialised laboratory techniques, not low-cost commercial processes.

A low-cost ceramic-metal functionally graded material would be ideal for wear-resistant linings in the mineral processing industry. Such a material would comprise a hard ceramic face on the exposed side, a tough metal face on the rear side that can be bolted or welded to a support frame, and a graded composition from metal to ceramic in between. The gradation would enhance the toughness of the ceramic face and also prevent ceramic-metal debonding. Such a material would uniquely combine the following attributes: high abrasion resistance (ceramic face), high impact resistance, and convenience: weldable/boltable to metal supports.

There would be little point in developing such a material unless it could compete commercially with the wear-resistant ceramics currently on the market, which range from tens to hundreds of dollars per kilogram, with alumina at the bottom end and imported tungsten carbide at the top end

of this range. Unless this can be achieved, the potential benefits of bulk wear-resistant tiles of metal-ceramic FGMs will remain an unrealised possibility.

Finally, a controlled-blending process has been developed recently for the fabrication of functionally graded materials of broad regular gradient. This is known as the impeller dry blending process (IDB). The IDB process is characterised by the following features:

— low-cost process,
— rapid throughput rates (hundreds of grams per minute),
— broad gradients millimeters to centimeters in breadth,
— regular and continuous (not layered) gradients are achievable with a high level of control over gradient profile.

In controlled blending, the two FGM components are blended during forming and the ratio is continuously varied from 100% component 1 through to 100% component 2 (or variation thereof). This approach potentially offers the unique advantage of being able to produce precisely controllable regular functional gradients independent of the system-inherent issues of powder density and gravitational settling mechanisms. Also, unlike segregation, controlled blending enables very rapid processing rates. To date, controlled-blending has mostly been used for making FGM thin films. For example, FGM thin films by thermal spraying (blended powder feed), vapor deposition (CVD/PVD blended gas feed), electrophoretic deposition (blended slurries), filter pressing (blended slurries), and blended spray drying.

The objective of the next part of the present study is one of the most promising, non-destructive research technique called X-ray texture tomography (XTT). The XTT was elaborated reacently in the Institute of Metallurgy and Materials Science of the Polish Academy of Sciences in Kraków.

Texture investigation of the FGMs

Non-destructive testing of materials with laminar and gradient structure is one of priority research of temporary materials engineering in reference to near-the-surface areas. In that field crystallographic texture and residual stresses analysis in near-the-surface areas of structural elements become more and more useful. Crystallographic texture is a statistical property of a material with crystalline structure manifested by the ordering of the spatial orientation of the particular crystallites (grains, sub-areas and particles). The texture favours the anisotropy of the physical properties of polycrystalline materials, so strongly manifested in the FGMs

Recently introduced and verified experimentally the *X-ray texture tomography* (XTT) represents a non-invasive method of investigating the texture of the near-the-surface areas on X-ray penetration depth, usually up to *100* μm. It allows to localize the texture changes occurring under the sample surface to a certain definite depth. XTT consists in the registration of the diffraction effects according to a definite method and their transformation according to the developed procedure utilizing the

available calculation methods. As a result an information set is obtained helpful at the interpretation of various structural effects, quality control of deposited coatings and in designing the production technology of new materials of specific properties. Such materials and composites are as a rule structurally inhomogeneous and are numbered among modern class materials like the FGMs. Their physical properties depend to a great extent on texture, the effective analysis of which can be carried out only in a way not disturbing the subtle arrangement of the layers, formed most often deliberately in a technologically advanced process.
Using texture tomography it is possible to investigate such problems as; anisotropy of physical properties, inhomogeneity and heredity of texture, distribution of residual stresses, fatigue wear of surface.

In spite of some limitations, the XTT adds the missing element to make the set of the research tools of the microstructure and supplements the electron microscopy wherever the scale of the examined phenomenon is beyond the nano-metric area. An essential of this research procedure is the possibility of its automatization which facilitates its application not only in scientific laboratories but also in industry.

The chapter presents a basis of the XTT and example of its application in study of structure of the FGMs considering their importance for the present-day materials engineering. Application of the proposed method in crystallographic texture analysis of various materials with non-homogeneous structure, like protective Zn layer deposited on the deep drawing steel, the Si/HfN electronic composition, and Ti/TiN coating of a polyurethane substrate are presented.

About the X-ray texture tomography

To describe of the crystallographic texture of a sample of a given material, appropriate research methods are developed in the home Institute for over 40 years. Although many experimental techniques and calculation methods of texture analysis are known, there is no effective way of texture investigation in the near-the-surface areas. The introduced *X-Ray Texture Tomography* seems one of the most effective in this field.

The XTT is a non-destructive method of texture analysis in the near-the-surface area, which diameter is determined by penetration depth of the applied radiation. The method consists in a specific manner of the registration of the experimental data and their mathematical transformation by introduced procedures. The notion of pole figure $P_{(hkl)}(\alpha,\beta)$, used in the analysis of texture, indicates a two-dimensional, equiangular stereographic projection of poles of crystallographic planes $\{hkl\}$ on a chosen projection plane, e.g. the sample surface. The parameters of such a projection are two angles, α and β, which determine the position of the projections of poles, the density of which reflects the intensity of figure at the given point (Cullity, 1978, Bunge, 1982a)[5].

The diffraction signal, recorded by the reflection method as the intensity of a deflected beam, carries information about the structure of the near-the-surface layer of some measurement method of the pole figure by the reflection method of Schulz (1949) is characterised by varying information depth. The information depth, however, can be controlled during the experiment, among other things, by means of additional inclination of the sample. This allows retaining stable information depth

at a chosen level in some definition fragment of the pole figure recorded by the Schulz's reflection method. At the adopted assumptions, the only and sufficient condition to keep stable the information depth is to maintain constant, strictly defined angle of incidence of the beam on the sample during the measurement. This condition can be satisfied, for example, by selecting appropriate values of the goniometric angles (ω,χ,φ) for each point (α,β) of the measured figure. The figure recorded in such measurement conditions has been called *constant-depth pole figure*. Figure 2 shows the changes in the information depth accompanying the inclination of the sample (the angle χ) during the measurement of normal (averaged) and constant-depth pole figures.

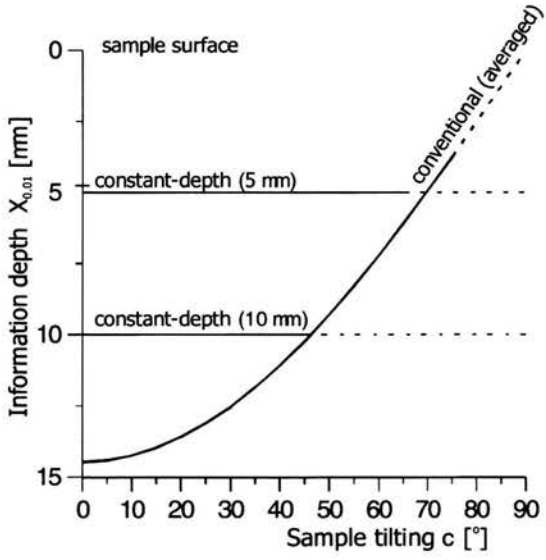

Fig. 2. *Change of the information depth as a function of the sample tilting angle χ for Cu (111) pole figure, measured in a conventional way by the reflection method, and for constant-depth pole figures with 5 μm and 10 μm information depth. Filtered CoKα radiation was applied. Broken lines indicate the non-measurable range of figures in the applied experimental conditions*

Registration of the *constant-depth* pole figures can be realised only when a constant incidence angle of the beam on the sample is retained, which is made possible using the texture goniometer with the option of expansion of the scanning mode $\theta \leftrightarrow 2\theta$ to the $\omega \leftrightarrow 2\theta$ one.

The inclination of sample χ in the conventional (symmetric) measurement geometry of Bragg-Brentano ($\omega = 0$) causes that each "circle" (α = *const.*) on a pole figure measured in such conditions corresponds to a different information depth ($X_{0,01}$), and simultaneously to another average texture, in accordance. If the texture is inhomogeneous, as in the FGMs, the described pole figure becomes intrinsically contradictory, and therefore it does not represent an appropriate set of data for the reproduction of a reliable three-dimensional orientation distribution function.

Changing the inclination of the sample χ and ω it is possible to calculate the profile of the information depth of the reflection *hkl*, called further on the *information valley*. An example of such an information valley for *111-Cu* reflection is shown in Fig.3. As it is indicated in the figure, it is possible to maintain the measurement conditions along a constant-level "path" of such a profile, i.e. a constant information depth.

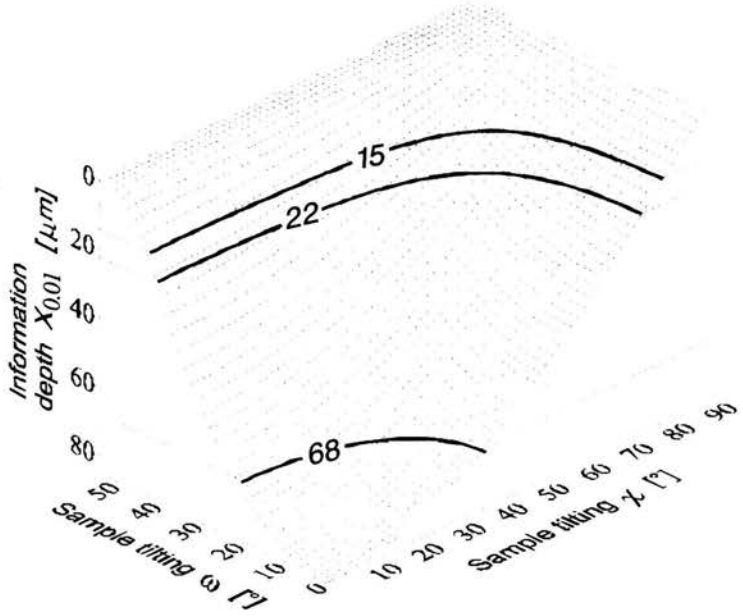

Fig. 3. *The information valley (information depth $X_{0.01}$ versus sample tilting ω and χ angles) of X-ray CoKα radiation for the 311 Bragg reflection in Al sample. The izo-depth geometrical conditions lines for registration of 15 μm, 22 μm and 68 μm single-layer (311) pole figures are marked*

The curve shown in Fig. 2 for a standard pole figure (*111*) is a one-dimensional section of the profile from Fig. 3 along the line $\omega = 0$. Figure 4 shows the selected paths $\omega = \omega(\chi)_{\xi = const.}$ of the information valley for constant-depth pole figures of *Al* and *CoK*α beam, calculated for various $X_{0,01}$ values. For each figure there are also given the constant values of the angle of the beam incidence on the sample which must be retained during the registration of constant-depth pole figures.

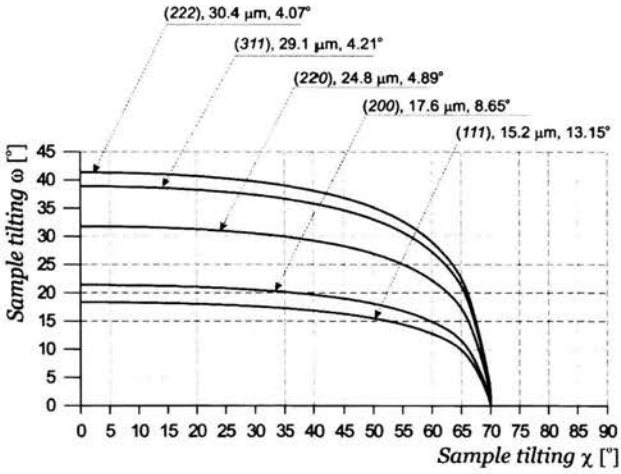

Fig. 4. *Curves $\omega = \omega(\chi)\xi$ determining the measurement conditions of constant-depth pole figures for aluminium, which can be registered in the variation range of the angle χ from 0 to 70°. The particular figures (hkl) have been denoted exceptionally with the indices of Bragg's reflections on which the measurement is based. For each figure there are given its information depth (in μm) and the value of the constant angle of incidence of the sample which must be preserved during the measurement*

In the symmetric focusing system of Bragg-Brentano the reference systems of the sample and the projection plane for a pole figure are identical, the result of which is a direct relation between the angles describing the orientation of the diffraction vector in both systems: $(\chi,\varphi) \Rightarrow (\alpha,\beta)$. This relation is used for the construction of a standard pole figure basing on the measurement data (Cullity, 1978; Bunge, 1982a).[5,4]

Changes in the orientation of the diffraction vector in an asymmetric focusing system, used in the described method of measuring constant-depth pole figures are realised through a combination of three angles (ω,χ,φ) according to the scheme presented in Fig. 3. Introduction of an

additional angle ω in relation to the symmetric geometry is responsible for the fact that the co-ordinates of the pole figure in the sample system cannot be expressed directly by the co-ordinates of the diffraction vector in this system. This means that the registered pole figure can be represented in the sample system, however only after carrying out an appropriate transformation of the co-ordinates of this vector (Bonarski et al., 1998a)[2]. In Fig. 5 there are presented the geometric dependences between the co-ordinates of the diffraction vector in the goniometer system and in the sample system, as well as appropriate (equi-axial) stereographic projection, which is a basis for the construction of constant-depth pole figures.

Applying the methods of spherical geometry (Bronsztejn and Siemiendiajev, 1959)[3] and making use of indication by letters, given in Fig. 5, there have been derived mathematical relations which enabled to carry out the transformation of the angular co-ordinates.

$$\alpha = \arccos\left(\cos\chi \cdot \cos\left(\arcsin\left(\sin\omega \cdot \cos\chi\right)\right)\right) \qquad 1a$$

$$\beta = \varphi + \arcsin\left(\sin\omega \cdot \frac{\sin\chi}{\sin\alpha}\right) \qquad 1b$$

where $-\frac{\pi}{2} < \omega < \frac{\pi}{2}$ and $0 \leq \chi < \frac{\pi}{2}$.

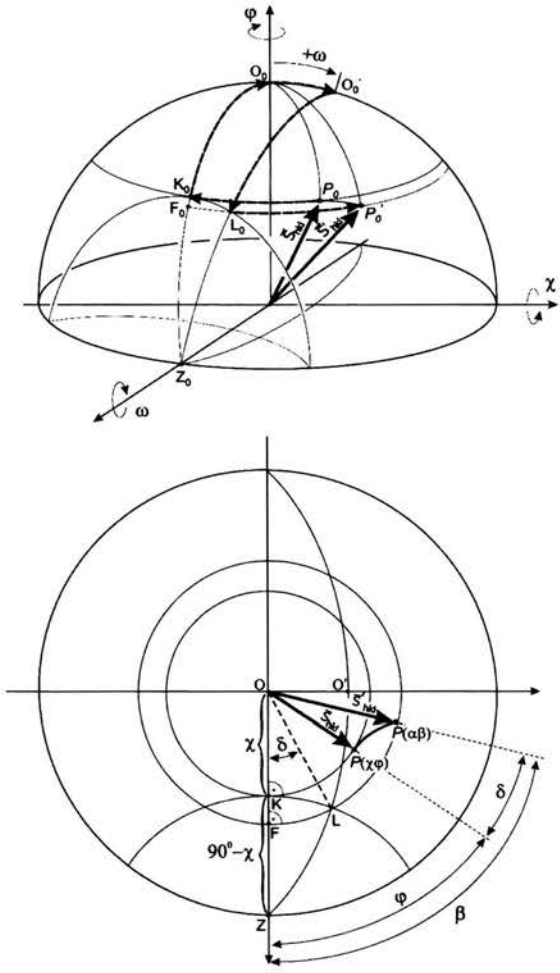

Fig. 5. *Illustration of the transformation of the goniometer co-ordinates (ω,χ,φ) to the system of the pole figure (α,β) for positive values of the angle ω*

As it follows from the above equations, the transformation of the co-ordinates $(\omega,\chi,\varphi) \Rightarrow (\alpha,\beta)$ does not depend on Bragg's angle $\theta_{(hkl)}$, which is the consequence of the definition of the angle ω with respect to the symmetric orientation of the sample in the Bragg-Brentano measurement system. Equations (1a) and (1b) determine the way in

which the angles of inclination of the sample ω and χ related by the equation: $\omega = \omega(\chi)_{\xi=const.}$ depend on each other during the measurement of constant-depth pole figures with constant information depth.

Due to this transformation the measurement lattice $\Delta\chi,\Delta\varphi$ becomes twisted into a spiral in relation to the lattice of the co-ordinates of figures $\Delta\alpha,\Delta\beta$, as shown in Fig. 6. Moreover, in the middle of the figure a *blind area* is formed (with its radius equal to the value of the angle ω for $\chi = 0$) for which the data cannot be registered in asymmetric conditions, i.e. $\omega = \omega(\chi)_{\xi=const.}$

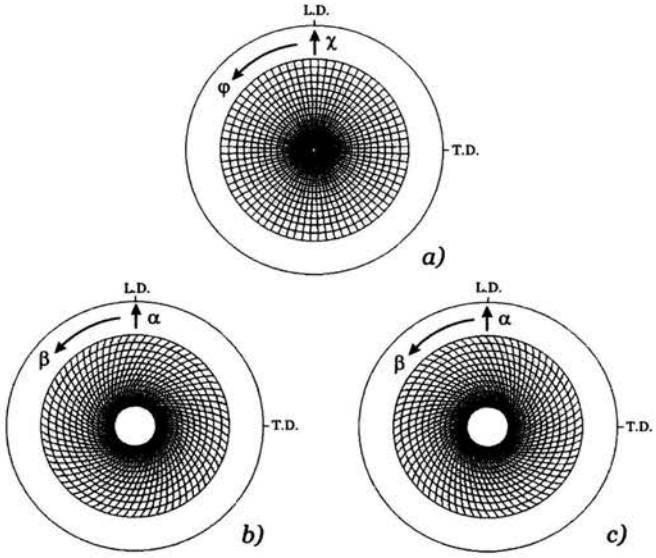

Fig. 6. *Transformation of the goniometer co-ordinates (χ,φ) from an equiangular measurement network ($\Delta\chi,\Delta\varphi$) in the asymmetric system (a) to the pole figure co-ordinates (α,β) in a symmetric system. The measurement (and the transformation) conditions refer to a constant-depth pole figure (111) Al with 15 μm information depth, obtained at positive (b) and negative (c) values of the angle ω. The visible "blind" areas in the central part of the pole figures are of the same dimensions and do not depend on the sign of the angle of "retreat" from the Bragg-Brentano conditions*

The registered constant-depth pole figure is thus incomplete both on the boundary within the range of the angle α close to $90°$ and in the middle part in the range α close to 0 (Fig. 6). If the incomplete areas are appropriately small, it is possible on the basis of such pole figures to calculate the orientation distribution function (Bunge, 1982a; Pawlik, 1986; Pawlik and Pospiech, 1986; Dahlem-Klein et al., 1993)[4,13,14,6]. In this sense, the admissible size of the incomplete areas depends on the number and type of the measured figures, which result from the symmetry of the crystallographic system of the material. This determines simultaneously the extent of application of constant-depth pole figures in the quantitative texture analysis of functionally graded materials, which are the subject of the introduced method of X-ray texture tomography.

Experimental verification of the method has been carried out and its effectiveness estimated using a reference sample of known texture with accurately defined inhomogeneity. An example of the registered constant-depth pole figure and its processed forms are shown in Fig. 7.

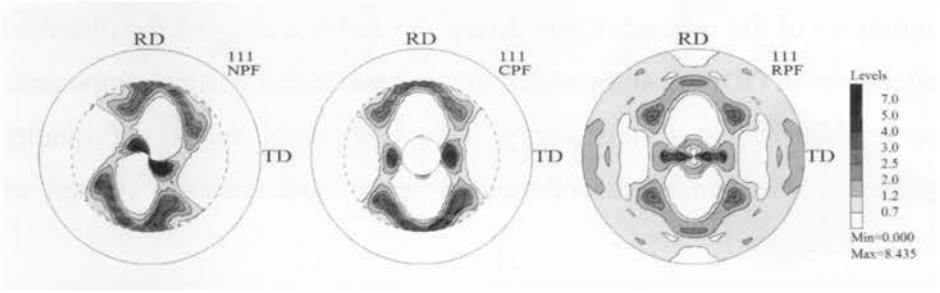

Fig. 7. *Constant-depth pole figure (111) with constant information depth $X_{0,01}$ = 15 μm for the first tomographic layer of a composite Al-reference sample: (left) experimentally registered, (centre) after transformation by the XTT procedures and (right) calculated from the reconstructed orientation distribution function*

The orientation distribution function obtained in the conventional way, i.e. based on the traditionally measured pole figures does not enable to reproduce the depth profile of the texture changes in examined microstructure area of the FGM. Such an analysis is made possible by texture tomography which is shown in Fig. 8. Besides the texture function for the tomographic layers there is also presented the image of the averaged orientation distribution, supplied by the conventional method of texture analysis in which the texture inhomogeneity is not taken into consideration.

A comparison of results obtained from the texture tomography of the *Al*-reference sample (Fig. 8) and computer simulation (*Bonarski, 2001*)[1] allows to formulate the evaluation of the quality of the method in terms of its accuracy, precision and repeatability.

Accuracy – the observed relatively small differences in the proportions of the volume fractions of the components of inhomogeneous texture in the particular tomographic layers are due to considerable divergences of the thickness of tomographic layers, selected with the purpose to estimate the limitations of the method. Considering the above causes of the observed differences in ODF it can be stated that the particular texture components are reproduced in a satisfactory way, both with respect of quality (maximum position in the orientation space) and quantity (values of texture functions).

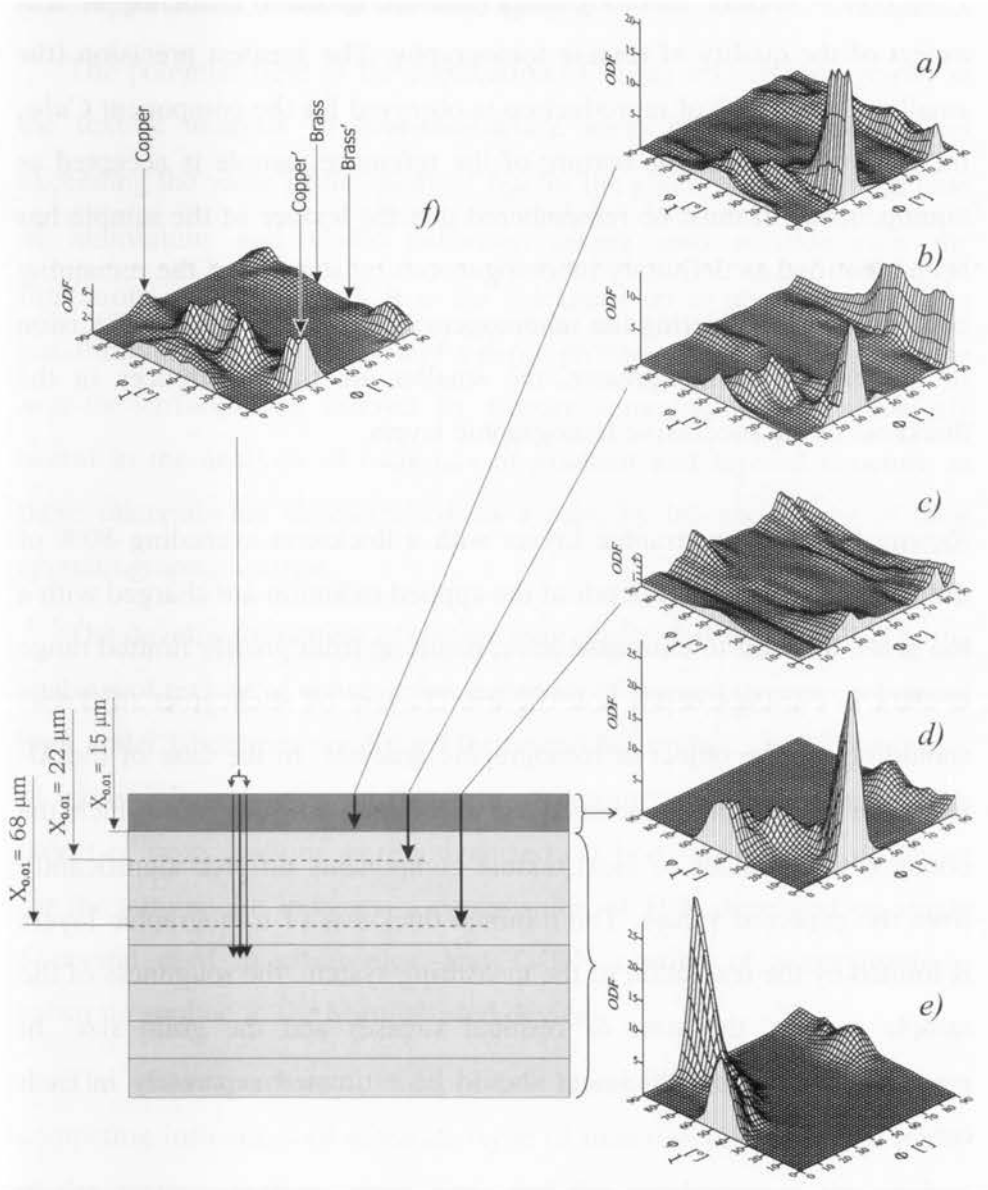

Fig. 8. *Tomographic layers in the Al-reference sample and their texture presented in the form of ODF sections for the angle $\varphi_2 = 45°$: (a) layer $X_{0,01} = 15$ µm, (b) layer $X_{0,01} = 22$ µm, (c) layer $X_{0,01} = 68$ µm, (d) texture of the sample surface layer (measured separately), (e) substrate texture (measured separately), (f) sample texture obtained on the basis of conventional measurements (averaged)*

Precision – texture inhomogeneity has the greatest influence of this aspect of the quality of texture tomography. The greatest precision (the smallest dispersion) of reproduction is observed for the component *Cube*, on account of which the texture of the reference sample is accepted as homogeneous. It must be remembered that the texture of the sample has been identified as definitely inhomogeneous on account of the remaining components. Considering the inhomogeneity of the texture, the precision of the method is the greater, the smaller are the differences in the thickness of the successive tomographic layers.

Repeatability – tomographic layers with a thickness exceeding *80%* of the effective penetration depth of the applied radiation are charged with a too great, difficult to eliminate error, resulting from greatly limited range of data in constant-depth pole figures. Layers of such great thickness should not be the object of tomographic analysis. In the case of the *Al*-reference sample this concerned the layer $X_{0,01} = 68\ \mu m$, for which the obtained ODF values of most texture components differed significantly from the expected values. The minimal thickness of tomographic layers is limited by the resolution of the measuring system, the roughness of the sample surface, the state of residual stresses and the grain size. In practice, the minimal thickness should be estimated separately in each case.

2.2. Application of texture tomography

The potential field of the application of X-ray texture tomography is the texture analysis of near-the-surface areas of their thickness not exceeding the value of the quotient $1/\mu$ for the given material. In the case of aluminium and Co$K\alpha$ radiation, taking into consideration the limitations of the method, it is the thickness up to about $65\ \mu m$. The possibility of the reproduction of a depth profile of texture changes in the near-the-surface area offered by texture tomography, is particularly useful in the analysis of materials of gradient and layered structure as these materials are characterised, as a rule, by inhomogeneity of their crystallographic texture.

The developed method of texture tomography has been applied in the analysis of texture of construction materials of layered structure, obtained both under laboratory conditions for research purposes and in conditions of industrial production, in the form of definite structural element. The object of investigations were galvanized car body sheet metal produced for the automobile industry, a composition of HfN deposited on single *Si*-crystal used in electronics, and Ti/TiN coating of a polyurethane substrate applied in the heart assisted devices.

The microstructure of deposited layers is determined by the competing influences of substrate (type of material, condition and purity of the surface, texture, grain size) and the conditions of the applied deposition process. The newly forming texture of the first deposited areas (epitaxial growth) depends on the orientation of the substrate (heredity

effect). With increasing thickness of the layer the effect of the deposition conditions, which determine the inherent texture of the deposited layer, begin to dominate. In a similar way, under a strong influence of the substrate, there develop the residual stresses generated in the area of phase boundaries, as a result of the orientation difference and misfit of the crystallographic lattices of the substrate and the building up layer.

Galvanised car body sheet metal

One of the first layered composite examined by the XTT was galvanised car body sheet metal[1] (α-*Fe/Zn* system) in which the deposited layer was about *7.5* μm thick (Fig. 9). Applying the texture tomography, the orientation distribution function in a tomographic layer with the thickness *5.0* μm was reproduced. There were also registered conventional back-reflection pole figures, on the basis of which the ODF for the whole thickness of the deposited layer (*7.5* μm) and for the substrate to the depth of about *38* μm from the interface boundary was calculated.

The expected result of the performed texture tomography was to obtain information about the possible effect of the substrate on the inherent texture of the layer which is formed under industrial hydro-electro-chemical conditions of the deposition process. Selected $\varphi_2 = 45°$ cross-sections of the calculated orientation distribution

[1] *Deep-drawing steel sheet with a protective Zn layer, 7,5 μm thick, deposited in the process of electrolytic galvanising, was produced in T. Sendzimir Steel Works in Kraków (Poland).*

functions for the particular sample areas are shown in Fig. 10, together with the marked texture components.

The obtained results of texture tomography with respect to the system α-Fe/Zn can be summarised as follows:

The fibre components are the dominating ones in the texture of the deposited Zn layer. There have been identified relatively strongly developed components of {112}⟨uvw⟩ type, which become stronger and stronger with increasing the distance from the interface boundary. They dominate in the final texture formed in the applied deposition conditions (very high current densities, up to *30 A/cm*^{2}).

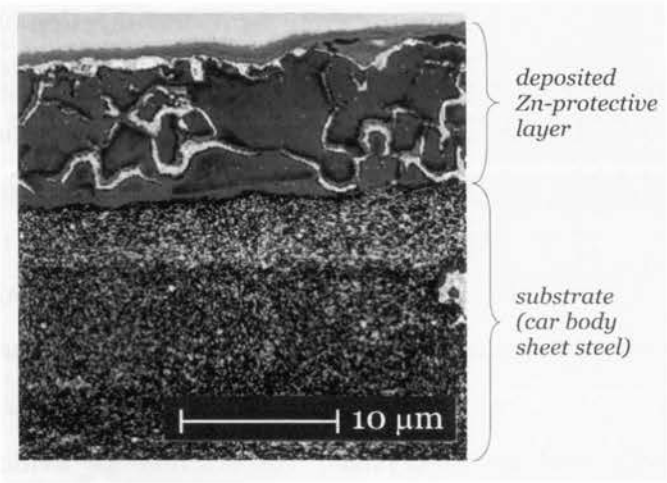

Fig. 9. *Microstructure of a cross-section of a galvanised car body sheet steel observed in a scanning microscope. The protective Zn layer, 7.5 µm thick, on a substrate of deep drawing steel is visible. [IMMS of PAN, Krakow]*

Preliminary evaluation of texture inhomogeneity made on the basis of a differential pole figure (*102*), suggests the occurrence of considerable differences in the texture at the thickness of the *Zn*-layer. The substrate texture is a typical texture of deep drawing car body sheet

metal, i.e. it is characterised by a great proportion of favourable component {111}⟨110⟩ and a small proportion of the component close to {001}⟨110⟩ one (Pańta and Karp, 1975; Lotter and Hougardy, 1978)[12,8]. In the ferritic structure of a car body steel *bcc*, there do not occur planes with such a dense arrangement of atoms as e.g. in *fcc* structure. The most densely occupied are here planes {*110*}. A much smaller density of atoms arrangement is demonstrated by planes {*112*}, whereas the occupation of atoms for the structure *bcc* is the greatest in directions ⟨111⟩. Taking into consideration the above characteristics and the identified texture components, it can be said that the direction normal to the sheet surface of the substrate represents the direction of the densest arrangement of atoms in the *α-Fe* lattice.

Most crystallites of the deposited *Zn*-layer of hexagonal structure (*c/a* = *1.856*), as it follows from its texture, become arranged in such a way that their {*112*} planes are approximately parallel to the substrate surface. In this way the most densely occupied planes {*001*} of these crystallites are not parallel to the most densely occupied planes {*110*} in *α-Fe* (see Fig. 11). However, a strong parallelism of the {*112*} and {*111*} planes in *Zn* and α-*Fe* crystals, respectively is evident. In this interpretation, the texture of *Zn*-layer with hexagonal lattice symmetry *hcp* inherits the texture of substrate with regular lattice symmetry *bcc*. The mentioned parallelism of the crystallographic planes implies automatically, that the most densely occupied directions ⟨*110*⟩ and ⟨*111*⟩ in the both type of crystals create relatively large angle of ca. *32°*.

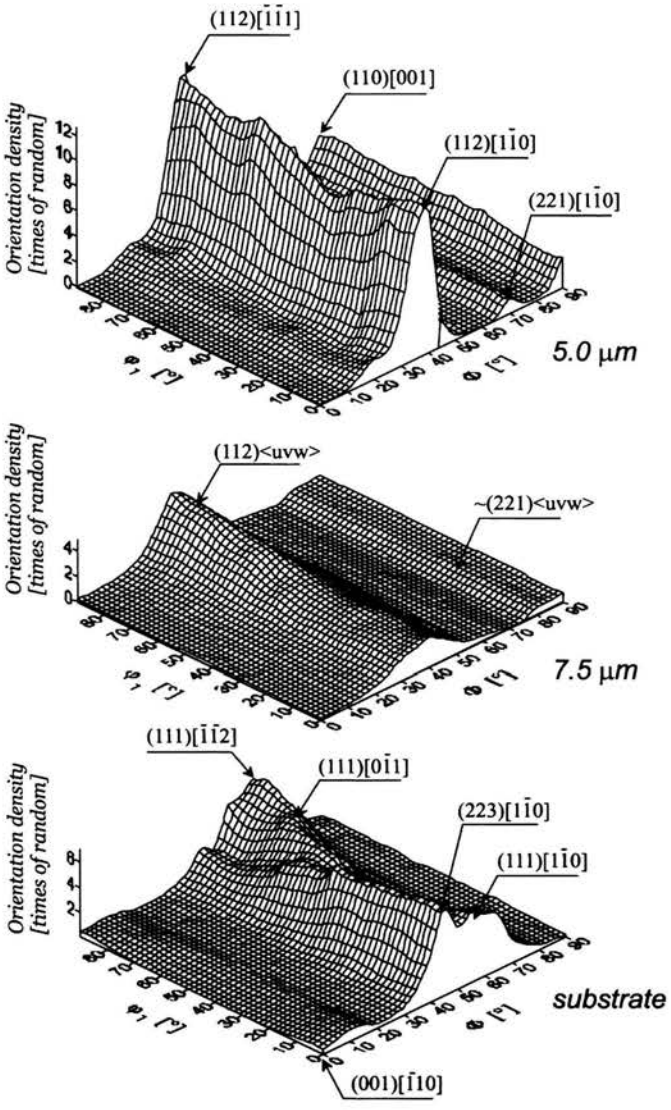

***Fig. 10.** Orientation distribution functions (sections $\varphi_2 = 45°$) for the near-the-surface layers, 5 μm and 7.5 μm thick in Zn coating and for the substrate (car body sheet steel), according to the denotations in the figure. Texture components dominating in the particular areas are indicated*

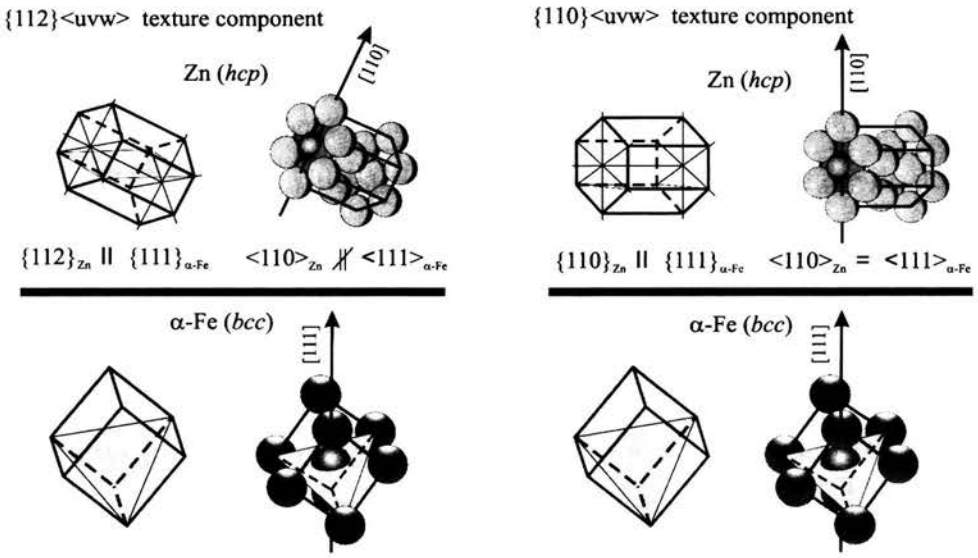

Fig. 11. *The scheme of crystallographic relations between substrate (α-Fe) and deposited layer (Zn) in the examined sample. Texture component of {112}⟨uvw⟩ type (left) and {110}⟨uvw⟩ one (right) are presented*

There exists, however, some part of the crystallites of the *Zn*-layer which are characterised by the orientation type of {110}⟨uvw⟩. This means that they are arranged with respect to the substrate in such a way that directions ⟨*110*⟩, most densely occupied with the atoms, are approximately parallel to directions ⟨*111*⟩, also most densely occupied, in the substrate, i.e. in *α-Fe*. It must be emphasized, that the mentioned orientation {110}⟨uvw⟩ is not the strongest texture component of the *Zn*-layer, and the described crystallographic dependence does not prevail in the overall substrate-layer relation. It follows from the texture image presented in Fig. 10 that this component is the not a consequence inheritance of the substrate texture by the *Zn*-layer. As it is clearly observed, a tendency to forming the {110}⟨uvw⟩ component increases

with growing distance from the *Zn/α-Fe* interlayer, especially above *2.5 μm* from this boundary. Simultaneously, the volume fraction of the {112}⟨uvw⟩ component becomes smaller in the final texture of the deposited *Zn*-layer.

Both the inherited component of {112}⟨uvw⟩ type and the extent of this effect have substantial influence, among other things, on the adhesion of the anticorrosive coating, such as the deposited *Zn*-layer, to the substrate.

Anisotropy of the drawability of car body sheet metal has been utilised in the production technology of structural elements obtained from this metal thanks to its proper texture {111}<110>. The deposited protective layer of *Zn* is the most durable the more its inherent texture is "adjusted" to the sheet metal texture, increasing the resistance of the final structural element to the exploitation conditions. These two requirements concerning the quality of the protective layer are satisfied when – on the one hand – the inheritance of the substrate texture is as strong as possible, and – on the other hand – the other surface of the layer demonstrates a texture which gives it higher resistance or, if it is possible – random distribution.

It can be concluded that the desired texture of the protective layer is inhomogeneous as a rule. As it is shown by the obtained results, the texture of the deposited *Zn*-layer is characterised by the essential inhomogeneity. The inheritance is distinct, although the main texture component (*fibre* type) of the *Zn*-layer {112}⟨uvw⟩ is the result of the $\{111\} \rightarrow \{112\}$ inheritance. The second component of {110}⟨uvw⟩ type, which dominates in the final texture of the layer is rather a result of

influence of the deposition parameters, and its eventual heredity should be excluded, in spite of parallelism of ⟨*110*⟩ *Zn* and ⟨*111*⟩ *α-Fe* directions (see Fig. 11).

There exist several technological parameters which enable to modify the texture of the deposited layers, and the texture tomography is a helpful in which the developed method has found one of the first applications in practice.

HfN on ⟨111⟩-oriented Si substrate

Layered structure composites like *Si/TiN* and *Si/HfN* are applied in electronics and precision industry on account of very good electronic properties and high tribological wear resistance of the outer layer. On account of a considerable misfit of the lattice parameters of the substrate and the deposited layer, in the area of the interface boundary there occur very strong inherent stresses whose values e.g. in the *Si/HfN* system reach *4.5 GPa*, which has a disadvantageous effect on the adhesion of the layer (Nowak 1999; Nowak *et al.*, 1999)[9,10]. To reduce the stresses, ion bombardment (e.g. with Si^+ ions) of the substrate immediately before the deposition of the layer is applied. The result is the formation of a strongly defected intermediate *Si*-layer which plays the role of an area relaxing the mentioned interfacial stresses. Accordingly, a *3*-layer system is formed whose properties vary along the thickness of the composite and are closely correlated with the changes of the microstructure and the crystallographic texture. Investigation of the texture of the systems under discussion requires the use of non-destructive methods, which do not

disturb the subtle system of the layers structure and the existing stresses. In such case the X-ray texture tomography can also be used.

In the laboratory of the Institute of Metallurgy and Materials Science of the Polish Academy of Sciences there has been carried out the analysis of texture of selected areas of $\langle 111 \rangle$-oriented *Si* single-crystalline system with defected surface layer on which a *HfN* layer of the thickness of about *500 nm* was deposited by the ion method[2].

The respective normal and constant-depth pole figures for HfN were registered by the back-reflection method of Schulz. The conventional pole figures contained data obtained from various information depths (about *500÷200 nm*) of the *HfN* layer depending on the Bragg's angle 2θ and the sample tilting angle χ. Constant-depth figures contained information from the tomographic layers of the thickness: $X_{0.01} = 200$ *nm*, $X_{0.01} = 400$ *nm* and $X_{0.01} = 500$ *nm*.

From the ODF image shown in Fig. 12 it follows that the texture of the near-the-surface area has axial character with the dominating component {111}<uvw>. A comparison of the orientation distribution functions for three tomographic layers confirms the texture inhomogeneity within the deposited layer. The texture of the tomographic layer $X_{0.01} = 500$ *nm* is the nearest to the average texture, which results from its thickness comparable with the thickness of the deposit as a whole.

---

[2] *The sample was fabricated at the Nagoya Institute of Technology, Dpt. of Electrical and Computer Engineering in Japan. A layer of HfN was deposited on the surface of Si-crystal with the orientation close to $\langle 111 \rangle$ by the technique of reactive sputtering. HfN has a regular symmetry of the crystallographic lattice (spatial group Fm3m) with the parameter $a_0 = 4.525$ Å and is of olive-brown colour. The Si/HfN sample showed orthorhombic symmetry.*

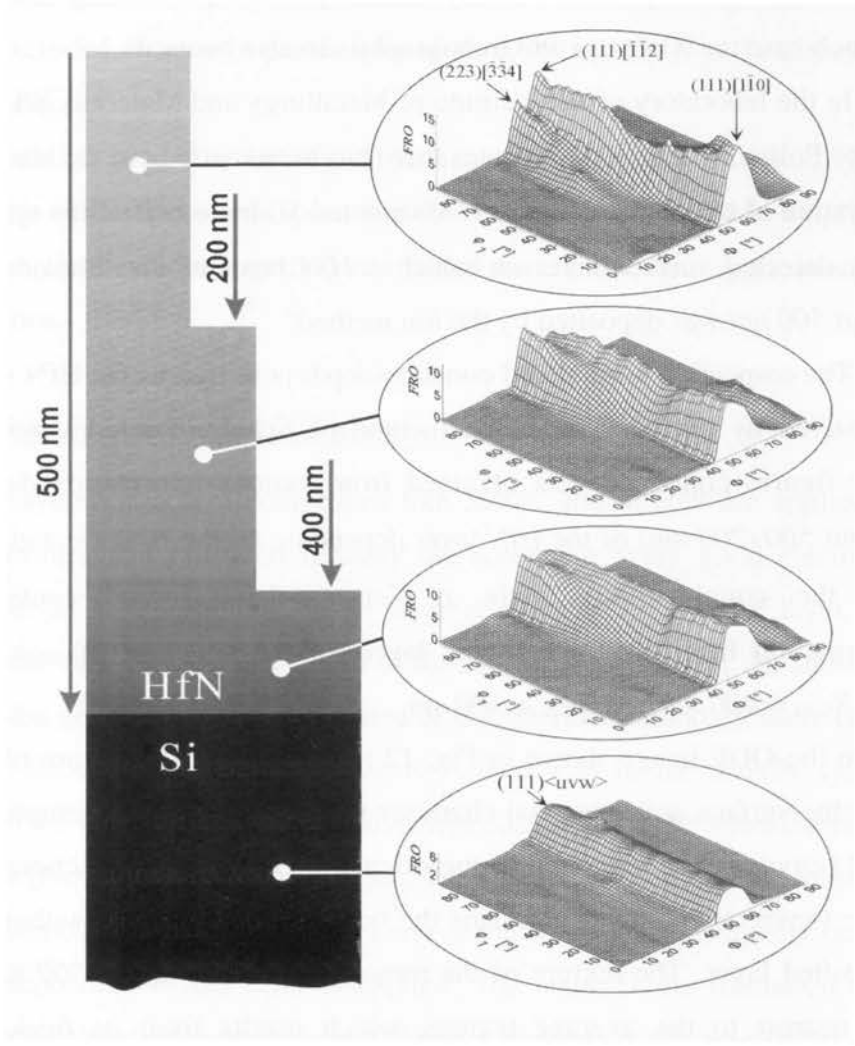

Fig. 12. *Texture tomography of a HFN layer, about 500 nm thick, deposited on ⟨111⟩-oriented Si crystal, presented in the form of ODF sections in the Euler angle space for $\varphi_2 = 45°$. The identified texture components for chosen tomographic layers of the thickness: 200 nm, 400 nm and 500 nm are indicated in the figure*

In the texture of areas more and more distant from the boundary *Si/HfN* there can be observed the components {223}<334> (dominating in the

layer $X_{0.01} = 400$ *nm*) and the component close to {111}<110> (dominating in the most outer layer $X_{0.01} = 200$ *nm*). The ODF values increase also in comparison with the averaged texture (Fig. 12). Such orientation distribution may be due to a considerable difference between the lattice parameters of *Si* and *HfN* (a_{Si} = 5.4282 Å, a_{HfN} = 4.5250 Å), which generates internal stresses[3], or maybe, to varying conditions of the deposition of successive areas of the *HfN*-layer. It may be assumed that the greatest stresses, thus also lattice disturbance, occur in areas localised near the interface boundary *Si/HfN*, and disappear as they move away from it. Hence, the scattering of the component {111}<uvw> in the near-the-surface area of *HfN* is smaller than that observed for this component identified almost in the whole thickness of the layer, which has been confirmed by ODF cross-sections for the successive tomographic layers, shown in Fig. 12.

Summarising the obtained results of the texture tomography of a layered system *Si/HfN* it can be stated that the texture of HfN layer, about *500 nm* thick, deposited on ⟨*111*⟩-oriented *Si* crystal is inhomogeneous and demonstrates distinct axial character {111}<uvw>. A strong effect of inheriting the substrate texture by the deposited layer has been observed. This effect is not uniform across the whole thickness of the layer. With increasing distance from the *Si/HfN* interface boundary it becomes weaker with simultaneous tendency for the formation of other components, e.g. {223}⟨334⟩ of the inherent texture in the *HfN*-layer.

[3] *The measurement of residual stresses for the same sample has confirmed their very high value, above 4.5 GPA in the HFN layer (Nowak et al. 1999)[10].*

Ti/TiN on *Ti*- and *Polyurethane*-substrate

Results of the XTT applied to texture analysis of a 3 μm thick *TiN* layer deposited on a *Ti*-substrate by means of a laser ablation technique are given in Figs 13a and 13b. Crystalline orientation of the upper part of the deposit up to 2 μm depth exhibit strong component {111}⟨110⟩, and in texture of the whole 3 μm layer dominates the {100}⟨010⟩ orientation. It proof a strong texture inhomogeneity of the *TiN* layer. Its depth-profile changes when the deposit is more and more thick. Such character of texture is determined on one hand by it substrate-inheritance (predomination of ⟨111⟩ axis) and on the other hand by the parameters of deposition process (predomination of ⟨100⟩ axis). The consequence of the texture inhomogeneity of the *TiN* layer is a gradient nature of its properties, like adhesity to substrate, wear- and corrosion-resistance, bio-compatibility.

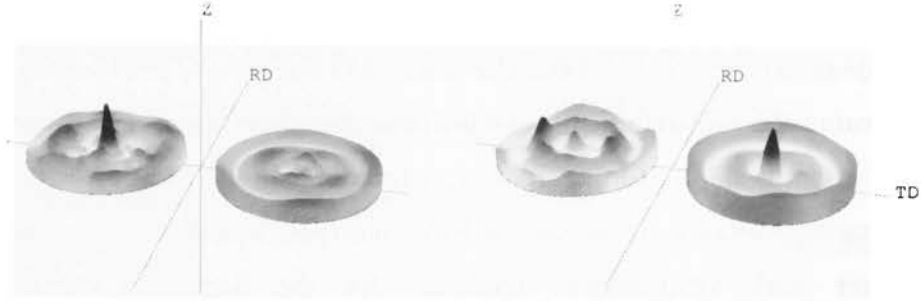

Fig. 13a. *3D view of the (111) constant-depth pole figures for 2 μm (left) and 3 μm (right) near-surface layers of TiN deposited on Ti-substrate*

Fig. 13b. *3D view of the (100) constant-depth pole figures for 2 μm (left) and 3 μm (right) near-surface layers of TiN deposited on Ti-substrate*

Analogical texture analysis was performed for a 3 μm thick *TiN* layer deposited on a *Polyurethane*-substrate (*PU*-substrate). In the case the texture inhomogeneity has been proved too, therewith the dominant components up to 2 μm depth and for the whole 3 μm layer were the same {112} <011> but developed to different extent (see Figs 14a and 14b). Moreover, a big size ⟨110⟩-oriented *TiN*-cluster was identified at the deeper part of the deposited layer.

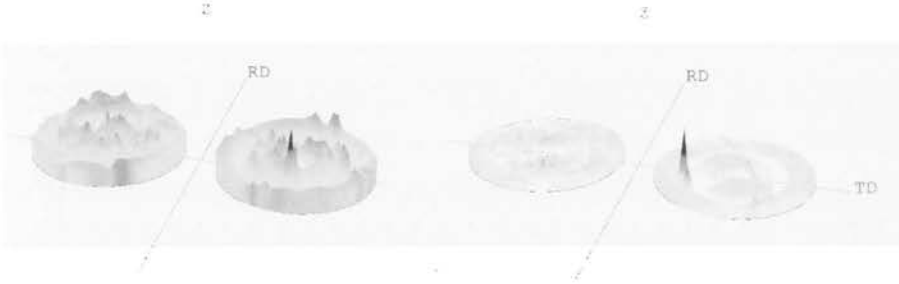

Fig. 14a. *3D view of the (111) constant-depth pole figures for 2 μm (left) and 3 μm (right) near-surface layers of TiN deposited on Polyurethane-substrate*

Fig. 14b. *3D view of the (100) constant-depth pole figures for 2 μm (left) and 3 μm (right) near-surface layers of TiN deposited on Polyurethane-substrate*

3. Final remarks

Technological processes involved in production of the FGMs lead to obtaining desirable physical properties of the materials or constructing elements, and are usually focused on bringing in appropriate changes in their internal structure. In principle, such structural changes on both nano- meso- and microscale affect the increase/decrease of crystal lattice defects, the changes of grains size/shape, the modification of phase composition and phase transition, the appearing or disappearing internal

stresses in the material, as well as the formation and/or modification of preferred crystallographic orientations (textures).

Usually, the structural analyses and studies of a material sample or a FGM-made structural element are carried out by means of elastic scattering techniqes (mostly x-ray diffraction and electron microscopy) in which appropriately prepared sample surface or chosen sample sections are thoroughly examined. Such measuring procedures enable obtaining quite representative and accurate results, as far as materials with homogeneous structure, properties and characteristics are concerned (e.g. fully isotropic crystallographic texture, homogeneous phase composition, residual strains, grain sizes or morphology). However, numerous advanced technologies of materials production and elements construction lead to the formation of so-called graded materials (structurally anisotropic) in which structure and properties inhomogeneities can not be neglected, and in some cases can even play a crucial role when designing novel objects or tools with more sophisticated properties. Among others, such materials processes like bonding the oxide ceramics(Al_2O_3 or ZrO_2) or nitride ceramics (Si_3N_4 or AlN) to metals, diffusive soldering, laser-aided depositing bio-compatible Ti(NC) layers, and many others, which offer new possibilities of fabricating novel materials and constructing elements with desirable structural properties and functionality, which will become interesting for technological applications.

In these cases, conventional measuring techniques and investigating methods (sufficient for homogeneous materials) become not satisfactory enough and the other, more sophisticated and much more precise ones, must be developed and employed. The texture analysis by the X-ray

texture tomography showed the effectiveness of the presented way of investigation of the FGMs. The XTT made possible to known to some extent the texture formation and controlling the properties of materials with the gradient structure.

The XTT enables to localize the texture changes in the near-the surface areas of the sample. It is particularly useful in texture analysis of gradient structures such as semiconductors, functional layers, protective coatings, solar cells, biologically functionalized surfaces on titanium implants for dental and orthopedic surgery, etc. By the XTT method, such research problems as anisotropy of the physical features, inhomogeneity and inheritance of texture, distribution of the residual stresses, fatigue wear can be investigated. The method complements the Electron Microscopy techniques everywhere the research problems exceed the nanometre scale.

References

1. Bonarski J. T. (2001). Rentgenowska Tomografia Teksturowa, Instytut Metalurgii i Inżynierii Materiałowej PAN, Kraków (in polish)
2. Bonarski, J.T., Bunge, H..J., Wciślak, L., Pawlik, K. (1998a). Investigation of Inhomogeneous Surface Textures with Constant Information Depth: Part 1: Fundamentals. Textures and Microstructures. **31**, No 1-2, 21-41
3. Bronsztejn, I.N., Siemiendiajev, K.A. (1959). Poradnik encyklopedyczny - Matematyka. tłum. z j.ros., PWN, Warszawa
4. Bunge, H.J. (1982a). Texture Analysis in Materials Science. Mathematical Methods. Butterworths Publ. London
5. Cullity, B.D. (1978). Elements of X-Ray Diffraction. 2nd Ed., Addison-Wesley Publ.Comp. Inc., London, Amsterdam, Don Mills, Sydney, Podstawy dyfrakcji promieni rentgenowskich. tłum z j. ang., PWN (1964), Warszawa

6. Dahlem-Klein, E., Klein, H., Park, N.J. (1993). ODF - Analysis for Cubic Crystal Symmetry Orthorhombic Sample Symmetry. Program System, Ed. H.J. Bunge, Cuvillier Verlag, Göttingen
7. Holt J. B., Koizumi M., Hirai T., Munir Z. A. eds. (1993). Functionally Gradient Materials, Ceramic Transactions, Vol. 34, Westerville, Ohio.
8. Lotter, W. and Hougardy, H.P. (1978). On the Formation of Texture in Deep Drawing Steels. Z. Metallkunde. 86, **3**, 164-170
9. Nowak, R. (1999). Mechanical Properties of Solids and Thin Films Studied by Depth-Sensing Indentation Method. Reports of Hiroshima University, R.78, Higashi-Hiroshima
10. Nowak, R. and Yoshida, F., Morgiel, J. and Major, B. (1999). Postdeposition relaxation of internal stress in sputter-grown thin films caused by ion bombardment. J. Appl. Phys. **85**, No 2, 1-12
11. Panda K. B. and Ravi Chandran K.S. (2003). Metallurgical and Materials Transactions, Vol. 34A, Sept. 2003.
12. Pańta, A, Karp. J. (1975). Badania tekstur blach głębokotłocznych ze stali 08X przy użyciu odwrotnych figur biegunowych. Hutnik. **11**, 430-435
13. Pawlik, K. (1986). Determination of the Orientation Distribution Function from Pole Figures in Arbitrarily Defined Cells. Phys. Stat. Sol. (b), **134**, 477
14. Pawlik, K. and Pospiech, J. (1986). Theoretical Methods of Texture Analysis. Proc. Workshop, ed. H.J. Bunge, (1986). Clausthall-Zellerfield
15. Schulz, L., G. (1949). A Direct Method of Determining Preferred Orientation of a Flat Reflection Sample Using a Geiger Counter X-Ray Spectrometer. J. Apply. Phys. **20**, 1030-1033